ELSEVIER

Polyhedron 21 (2002) 729–737

POLYHEDRON

www.elsevier.com/locate/poly

Structural studies of metal complexes of 2-pyridineformamide N(4)-methylthiosemicarbazone

Isabel García [a], Elena Bermejo [a], Ayman K. El Sawaf [b], Alfonso Castiñeiras [a,*], Douglas X. West [c]

[a] *Departamento de Química Inorgánica, Facultad de Farmacia, Universidad de Santiago de Compostela, E-15706 Santiago de Compostela, Spain*
[b] *Department of Chemistry, Faculty of Science, El Menoufia University, Shebin El-Kom, Egypt*
[c] *Department of Chemistry, 351700, University of Washington, Seattle, WA 98195-1700, USA*

Received 20 August 2001; accepted 4 December 2001

Abstract

Reduction of 2-cyanopyridine by sodium in dry methanol in the presence of N(4)-methylthiosemicarbazide produces 2-pyridineformamide N(4)-methylthiosemicarbazone, HAm4M. In the crystals of $[Ni(HAm4M)_2](ClO_4)_2\cdot 2H_2O$, $[Zn(Am4M)OAc]_2$ and $[Cd(HAm4M)Cl_2]\cdot DMSO$ the major ligand coordinates via its pyridyl nitrogen, imine nitrogen and sulfur atoms, the last of which forms a thione in the neutral ligand HAm4M and a thiolato group in $(Am4M)^-$. Both the acetato ligands in $[Zn(Am4M)OAc]_2$ are bis-monodentate bridges, which is unique among acetato-bridged binuclear complexes of thiosemicarbazones of this type. As in the complexes of other 2-pyridineformamide thiosemicarbazones, hydrogen bonds play an important role in these compounds. As well as by X-ray diffractometry, the new compounds were characterized by elemental analysis, FAB mass spectrometry and IR spectroscopy; in the case of the nickel(II) complex, by electronic spectroscopy and by molar conductivity and magnetic susceptibility measurements; and in the case of the zinc(II) and cadmium(II) complexes, by NMR spectroscopy (^1H, ^{13}C and, for Cd(II), ^{113}Cd). © 2002 Published by Elsevier Science Ltd.

Keywords: 2-Pyridineformamide; Thiosemicarbazone; Nickel(II); Zinc(II); Cadmium(II); Crystal structures

1. Introduction

The structures of a number of crystalline metal complexes of 2-pyridineformamide thiosemicarbazone (HAm4DH) have recently been studied [1–4], as have those of iron(III), cobalt(II) and nickel(II) complexes of 2-pyridineformamide N(4)-methylthiosemicarbazone, HAm4M [6] (Scheme 1). Spectra of copper(II) complexes of HAm4M have also been reported [5]. Having now obtained diffraction quality crystals of the binuclear zinc(II) complex $[Zn(Am4M)OAc]_2$, the cadmium(II) complex $[Cd(HAm4M)Cl_2]\cdot DMSO$ and the nickel(II) complex $[Ni(HAm4M)_2](ClO_4)_2\cdot 2H_2O$, we here compare their structures with those of the analogous compounds of HAm4DH and the previously reported metal complexes of HAm4M [6].

2. Experimental

2.1. Materials and instruments

All solvents used were reagent grade. $Ni(ClO_4)\cdot 6H_2O$ (Shering-Kalbaum), $Zn(CH_3COO)_2\cdot 2H_2O$ (ABCR), $CdCl_2\cdot H_2O$ (Aldrich), 2-cyanopyridine (Aldrich) and 4-methyl-3-thiosemicarbazide (Aldrich) were used with no further purification. HAm4M was prepared from 2-cyanopyridine as described previously [6]. Elemental analyses for C, H, N and S were performed on a Carlo Erba EA model 1108 elemental analyser. Melting points were determined in open tubes with a Büchi apparatus and are uncorrected. IR spectra were obtained in the 4000–400 cm^{-1} region using KBr pellets in a Mattson Cygnus 100 spectrometer, and in the 500–100 cm^{-1} region using polyethylene-sandwiched Nujol mulls in a Bruker IFS 66V spectrometer. ^1H and ^{13}C NMR spectra in DMSO-d_6 were run in Bruker AMX 300 and WM 300 instruments, respectively, using TMS as internal refer-

* Corresponding author. Tel.: +34-981-594-636; fax: +34-981-547-163.
E-mail address: qiac01@usc.es (A. Castiñeiras).

0277-5387/02/$ - see front matter © 2002 Published by Elsevier Science Ltd.
PII: S0277-5387(02)00835-5

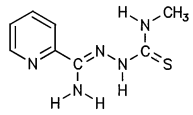

Scheme 1.

ence. The ^{113}Cd NMR spectrum of the cadmium(II) complex was run on a Bruker AMX 500 apparatus in dimethylformamide with D_2O as reference and is expressed relative to 0.1 M $Cd(ClO_4)_2$. Mass spectra (FAB, 3-nitrobenzyl alcohol, Xe, 8 kV) were obtained in a Kratos MS 50 apparatus equipped with a DS-90 data acquisition system. Solid state electronic absorption (diffuse reflectance) spectra were recorded over the 900–350 nm region in a Shimadzu UV–Vis/NIR UV-3101PC spectrophotometer. Magnetic susceptibility measurements were performed at 25 °C using a Johnson Matthey Alfa MSB-MK1 Gouy balance; the data were corrected for diamagnetic susceptibilities. Molar conductivities of 10^{-3} M solutions were measured with a WTW LF-3 conductivity meter.

2.2. Synthesis and crystallization of the complexes

The complexes were prepared by the following procedure. A solution of HAm4M (0.25 g, 1.19 mmol) in ethanol (20 ml) was added to a solution of zinc(II) acetate (0.26 g, 1.19 mmol), cadmium(II) chloride (0.22 g, 1.19 mmol) or nickel(II) perchlorate (0.22 g, 0.60 mmol; **caution, perchlorates are potentially explosive and should be handled carefully**) in 20 ml of 96% ethyl alcohol, and the mixture was stirred for several days. The resulting solids were filtered off, washed thoroughly with cold ethanol and dried over $CaCl_2$.

2.2.1. $[Ni(HAm4M)_2](ClO_4)_2\cdot H_2O$

Green; 0.265 g, 63.7%; m.p. 250 °C. MS (FAB): $m/z = 477$ $[Ni(HAm4M)_2]^+$, 443 $[Ni_4(HAm4M)]^+$, 385 $[Ni_3(HAm4M)]^+$, 268 $[Ni(HAm4M)]^+$. *Anal.* Found: C, 27.90; H, 3.30; N, 19.94; S, 9.65%. Calc. for $C_{16}H_{24}Cl_2N_{10}NiO_9S_2$ (694.18): C, 27.68; H, 3.48; N, 20.07; S, 9.24%. IR (KBr, ν/cm^{-1}): 3420, 3353, 3313, 3181 (N–H); 1679, 1573, 1483 [(C=N)+(C=C)]; 1133–1089 (ν_3, ClO_4); 1030 (N–N); 940–929 (ν_4, ClO_4); 790 (C=S); 636 (py). Far-IR (Nujol, ν/cm^{-1}): 417 (py); 339 (Ni–S); 243, 225 (Ni–N). UV–Vis (ν/cm^{-1}): 28 735, 26 525, 15 611, 11 337.

2.2.2. $[Ni(HAm4M)_2](ClO_4)_2\cdot 2H_2O$

Single crystals of $[Ni(HAm4M)_2](ClO_4)_2\cdot 2H_2O$ suitable for analysis by X-ray diffractometry were obtained by slow evaporation of the mother liquor in air at room temperature. *Anal.* Found: C, 26.96; H, 3.77; N, 19.66; S, 8.99. Calc. for $C_{16}H_{26}Cl_2N_{10}NiO_{10}S_2$ (712.20): C, 26.98; H, 3.68; N, 19.67; S, 9.00%.

2.2.3. $[Zn(Am4M)(OAc)]_2\cdot H_2O$

Yellow; 0.336 g, 82.6%; m.p. 225 °C. MS (FAB): $m/z = 332$ $[Zn(HAm4M)(OAc)]^+$, 273 $[Zn(HAm4M)]^+$. *Anal.* Found: C, 35.18; H, 4.14; N, 20.49; S, 9.48%. Calc. for $C_{20}H_{28}N_{10}O_5S_2Zn_2$ (683.38): C, 35.15; H, 4.13; N, 20.50; S, 9.38%. IR (KBr, ν/cm^{-1}): 3432, 3314 (N–H); 1644, 1582 (ν_{as}, CO_2); 1564, 1514, 1469 [(C=N)+(C=C)]; 1385 (ν_s, CO_2); 1014 (N–N); 791 (C=S); 638 (py). Far-IR (Nujol, ν/cm^{-1}): 410 (py); 321 (Zn–S); 288 (Zn–O); 254 (Zn–N). ^1H NMR (DMSO-d_6, δ/ppm): 2.82 (s, 3H, C8H); 6.35 (s,a, 1H, N4H); 6.89 (s, 2H, N5H); 7.57, 8.06, 8.47 (4H, py). ^{13}C NMR (DMSO-d_6, δ/ppm): 29.6 (C8), 119.9 (C2), 125.3 (C4), 39.6 (C3), 144.9 (C6), 146.2 (C5), 147.1 (C1), 175.3 (C7).

2.2.4. $[Zn(Am4M)(OAc)]_2$

Single crystals of $[Zn(Am4M)(OAc)]_2$ suitable for analysis by X-ray diffractometry were obtained by slow evaporation of the mother liquor in air at room temperature. *Anal.* Found: C, 35.98; H, 3.74; N, 21.49; S, 9.68. Calc. for $C_{20}H_{26}N_{10}O_4S_2Zn_2$ (665.37): C, 36.10; H, 3.94; N, 21.06; S, 9.64%.

2.2.5. $[Cd(HAm4M)Cl_2]\cdot H_2O$

Yellow; 0.324 g, 66.3%; m.p. 234 °C. MS (FAB): $m/z = 531$ $[Cd(HAm4M)_2]^+$, 357 $[Cd(HAm4M)Cl]^+$. *Anal.* Found: C, 23.69; H, 2.86; N, 16.99; S, 8.75. Calc. for $C_8H_{13}CdCl_2N_5OS$ (410.59): C, 23.40; H, 3.19; N, 17.06; S, 7.81%. IR (KBr, ν/cm^{-1}): 3473, 3343, 3209 (N–H); 1665, 1631, 1565, 1441 [(C=N)+(C=C)]; 1016 (N–N); 794 (C=S); 640 (py). Far-IR (Nujol, ν/cm^{-1}): 404 (py); 322 (Cd–S); 252 (Cd–N); 219, 182 (Cd–Cl). ^1H NMR (DMSO-d_6, δ/ppm): 2.95 (s, 3H, C8H); 6.91 (s, 2H, N5H); 7.62 N (s,a, 1H, N4H); 7.43, 7.76, 8.44, 8.55 (4H, py); 10.06 (s, 1H, N3H). ^{13}C NMR (DMSO-d_6, δ/ppm): 30.1 (C8), 121.1 (C2), 126.4 (C4), 138.2 (C3), 140.6 (C6), 146.0 (C5), 149.0 (C1), 176.5 (C7).

2.2.6. $[Cd(HAm4M)Cl_2]\cdot DMSO$

Single crystals of $[Cd(HAm4M)Cl_2]\cdot DMSO$ suitable for analysis by X-ray diffractometry were obtained by slow evaporation of a DMSO solution in air at room temperature. *Anal.* Found: C, 25.45; H, 3.61; N, 14.85; S, 13.59. Calc. for $C_{10}H_{17}CdCl_2N_5OS_2$ (470.71): C, 25.52; H, 3.64; N, 14.88; S, 13.26%.

2.3. Crystal structure determination

Data were collected from selected crystals mounted on glass fibres. The data for $[Ni(HAm4M)_2](ClO_4)_2\cdot 2H_2O$ were processed with SAINT [7] and corrected for absorption using SADABS (transmission factors: 1.000–0.732) [8]. For $[Zn(Am4M)OAc]_2$ and $[Cd(HAm4M)Cl_2]\cdot$DMSO, cell constants and orientation matrices for data collection were obtained by least-squares refine-

ment of the diffraction data from 25 reflections in the ranges $21.95^\circ < \theta < 45.72^\circ$ and $6.55^\circ < \theta < 10.81^\circ$, respectively, and semi-empirical absorption corrections were made (ψ-scans) [9]. The structures were solved by direct methods using the program SHELXS-97, and were refined by full-matrix least-squares techniques on F^2 using anisotropic displacement parameters [10]. Hydrogen atoms were placed at the calculated positions. Idealized H atoms were refined with isotropic displacement parameters set to 1.2 (1.5 for methyl groups) times the equivalent isotropic U values of the parent atom. Atom scattering factors were taken from the International Tables for X-ray Crystallography [11] and molecular graphics were produced using SCHAKAL [12].

3. Discussion

3.1. Synthesis and physicochemical properties

Reaction of the stated quantities of $Ni(ClO_4)\cdot 6H_2O$, $Zn(CH_3COO)_2\cdot 2H_2O$ and $CdCl_2\cdot H_2O$ with HAm4M in ethanol gave products of compositions $[Ni(HAm4M)_2](ClO_4)_2\cdot H_2O$, $[Zn(Am4M)OAc]_2\cdot H_2O$ and $[Cd(HAm4M)Cl_2]\cdot H_2O$, as shown by microanalytical. All three complexes are stable in air and are highly soluble in DMF and DMSO, less soluble in H_2O, MeOH, EtOH, MeCN and Me_2CO, and insoluble in $HCCl_3$ and toluene.

The mass spectra of the complexes all show peaks attributable to the species $[Ni(HAm4M)_2]^+$, $[Cd(HAm4M)_2]^+$ or $[Zn(Am4M)(OAc)]^+$ and, at lower m/z, to $[Ni(HAm4M)]^+$, $[Zn(Am4M)]^+$ or $[Cd(HAm4M)Cl]^+$; these species are common in the mass spectra of compounds of the form $[ML_n]X_m$ in which monovalent anions coordinate metals in oxidation states II or III [13]. The spectra also all contain peaks due to oligomeric species or ligand fragmentation (not listed), and the spectrum of the nickel compound shows peaks corresponding to multinuclear single-ligand species.

The IR spectrum of HAm4M has five strong bands in the range 4000–3000 cm^{-1}. Those at 3366 and 3234 cm^{-1} are due to the stretching modes $\nu_a(NH_2)$ and $\nu_s(NH_2)$, respectively; that at 3183 cm^{-1} to the hydrazinic NH; and the other two probably to thioamide NH stretching. The IR spectra of the nickel(II) and cadmium(II) complexes exhibit shoulders at 3420 and 3473 cm^{-1}, respectively, and broad bands at 3353–3313 and 3181 cm^{-1} (in the nickel complex) or 3343 and 3208 cm^{-1} (in the cadmium complex); all these bands probably arise from both the ν(OH) modes of the lattice water and the ν(NH) modes of the ligand. In the spectrum of the zinc(II) complex ν(NH) vibrations appear at 3431 and 3313 cm^{-1}, but there is no band corresponding to stretching of the hydrazinic NH, which is consistent with deprotonation of HAm4M. Neither does this spectrum show bands characteristic of thioamide or imino groups, which suggests that the ligand is coordinated in thiolato form, an interpretation that is further supported by the presence of a new band near 1514 cm^{-1} that seems to be due to the stretching mode of the conjugated >C=N–N=C< group (as in azines [14]) and hence implies that the sulfur is thiolic. The shift of the thiocarbonyl stretching mode from 797 cm^{-1} in HAm4M to lower frequencies in all the complexes is in keeping with coordination through sulfur [15], and the parallel shift of ν(C=N) from 1591 cm^{-1} to 1564–1578 cm^{-1} likewise corroborates coordination of the azomethine nitrogen [16]. Coordination of the pyridine nitrogen atom is less easily inferred from the pyridine bands, since the 1600–1400 cm^{-1} region is complicated by the presence of thioamide bands, but is clearly shown by the shift to higher frequencies of the deformation mode bands that appear near 625 and 405 cm^{-1} in the spectrum of HAm4M [17]. In the 400–100 cm^{-1} region the IR spectra of the complexes show bands that are not observed in that of the free ligand: a weak band in the range 340–320 cm^{-1} is attributable to ν(MS), bands in the range 260–220 cm^{-1} to ν(MN) vibrations [18], a band at 288 cm^{-1} in the spectrum of the zinc complex to ν(ZnO) [19], and two strong bands at 219 and 182 cm^{-1} in the spectrum of the cadmium complex to ν(CdCl) [20].

The molar conductivity of freshly prepared 10^{-3} M solutions of the nickel(II) compound in DMF, 166.9 S cm^2 mol^{-1}, corresponds to a 1:2 electrolyte [21]. The effective magnetic moment determined at room temperature is 3.18 MB, which is typical of high-spin octahedral complexes [22]. The diffuse reflectance spectrum is typical of hexacoordinate compounds of nickel(II) [22]. In the visible and near-IR regions, a low-energy band at 11 340 cm^{-1} can be assigned to the $^3A_{2g}(F) \rightarrow {}^3T_{2g}(F)$ transition (ν_1), and the band at 16610 cm^{-1} to the $^3A_{2g}(F) \rightarrow {}^3T_{1g}(F)$ transition (ν_2); the ν_3 band, which corresponds to the transition $^3A_{2g}(F) \rightarrow {}^3T_{1g}(P)$, is masked by the high-intensity charge transfer bands at 26 525 and 28 735 cm^{-1}. The first CT band probably reflects a metal–ligand CT transition, whereas the second is probably the result of an intraligand transition.

In the ^1H NMR spectrum of the zinc complex the nonappearance of the N3H signal (at 10.03 ppm in the free ligand) shows that the ligand is deprotonated in DMSO solution. The deshielding of N4H is probably due to withdrawal of charge from N4 as the result of an increase in charge delocalization upon complexation through the thiocarbonyl sulfur atom; the shielding of the N4 methyl protons is attributable to the same mechanism. In the cadmium complex the persistence of the N3H signal shows that this proton is retained in DMSO solution; the downfield shifts of the N3H and

N4H signals are attributable to coordination through the azomethine nitrogen atom and thiocarbonyl sulfur atom, respectively, and/or to the formation of hydrogen bonds between N3H (and to a much lesser extent N4H) and solvent.

In the ^{13}C NMR spectra of the zinc and cadmium complexes the shielding of C7 and C8 is attributable to a combination of the inductive effect of the metal and the move towards the thiol form induced by deprotonation (in the zinc complex) or coordination through the sulfur atom (in the cadmium complex). The shift of the C6 signal to higher field in the cadmium complex is in consonance with coordination through the azomethine nitrogen atom, but in the zinc complex an increase in electronic delocalization in the thiosemicarbazone moiety moves this signal to lower field. Coordination through the pyridine nitrogen atom is pointed to by the shielding of the pyridine C5 signals [15].

The ^{113}Cd NMR spectrum shows a single signal at 385.5 ppm. The fact that the metal atom is less deshielded than in $CdCl_2$ in DMSO [23] is consistent with data for other complexes of cadmium(II) chloride with thiosemicarbazones, and is compatible with pentacoordination of the metal [2].

3.2. Crystal structures

Table 1 summarizes crystal data and data collection details for the complexes $[Ni(HAm4M)_2](ClO_4)_2\cdot 2H_2O$, $[Zn(Am4M)OAc]_2$ and $[Cd(HAm4M)Cl_2]\cdot DMSO$. Selected bond lengths are listed in Table 2, and bond angles in Table 3. Perspective views of $[Ni(HAm4M)_2](ClO_4)_2$, $[Zn(Am4M)OAc]_2$ and $[Cd(HAm4M)Cl_2]$ are shown in Figs. 1–3, respectively. Intermolecular hydrogen bonding parameters are compiled in Table 4, and least-squares mean-plane data in Table 5.

3.2.1. Structure of $[Ni(HAm4M)_2](ClO_4)_2\cdot 2H_2O$ (1)

The crystal structure of planar, tetracoordinate $[Ni(Am4M)(OAc)]\cdot H_2O$, in which HAm4M has lost its N3 hydrogen, was described previously [6]. The structure of $[Ni(HAm4DH)_2](NO_3)_2$, where HAm4DH is 2-pyridineformamide thiosemicarbazone, has also been solved, and $[Ni(HAm4DH)(Am4DH)]ClO_4$ has been synthesized by reaction of HAm4DH with nickel(II) perchlorate [3]. We are therefore able to compare the coordination of neutral HAm4M with that of anionic Am4M and with similar complexes of HAm4DH.

In $[Ni(HAm4M)_2](ClO_4)_2\cdot 2H_2O$ the two ligands coordinate in the expected meridional conformation via the pyridine nitrogen, imine nitrogen and sulfur atoms. The N12–Ni1–N22 angle involving the imine nitrogens of the two ligands is 173.1(3)°, showing less distortion from octahedral symmetry than in $[Ni(HAm4DH)_2](NO_3)_2$, in which this angle is 169.6(2)° [3]. The other two *trans* angles, each of which involves the terminal donors of one of the tridentate ligands, are approximately 159.5°.

As in all 2-pyridyl thiosemicarbazones, the $Ni–N_{im}$, $Ni–N_{py}$ and Ni–S bonds increase in length in that order. The differences between the two ligands as regards these bond lengths are within twice their combined esds. Coordination does not significantly affect the imine C=N bond length, and the C=S bond is shortened only very slightly, from an average 1.699(5) Å to an average 1.680(9) Å (probably due to the loss of intermolecular hydrogen bonds present in HAm4M [6]). The other bonds of the coordinated thiosemicarbazone moiety are also similar in length to those found in HAm4M. The bond angles of the thiosemicarbazone moiety are altered somewhat upon coordination; the largest change affects N13–C17–S1 and N23–C27–S2, which average 122.5(2)° in $[Ni(HAm4M)_2](ClO_4)_2$ as against 120.0(4)° in HAm4M [6].

All of the coordinating bonds are, as expected, longer than in [Ni(Am4M)(OAc)] [6], which is tetracoordinate. The C17–S1 and N13–C17 bonds are significantly shorter than in [Ni(Am4M)(OAc)], but the C16–N12 bonds of the two compounds have the same length. As expected, there are significant differences between the bond angles of coordinated HAm4M and the coordinated N3-deprotonated anion [6].

The extensive hydrogen bonding in $[Ni(HAm4M)_2](ClO_4)_2\cdot 2H_2O$ involves the perchlorate ions, the water molecules, and all the uncoordinated nitrogens (Table 4). N14–H14 binds two oxygens belonging to the same perchlorate ion (one more strongly than the other), and ligand 1 binds the O1#1 water molecule via two different NH groups (N13–H13 and N15–H15A), but ligand 2 only forms hydrogen bonds with perchlorate oxygen.

The angle between the least-squares planes of the pyridine ring and the thiosemicarbazide moiety in $[Ni(HAm4M)_2](ClO_4)_2$ averages 5.5(4)° {cf. 11.0(2)° in $[Ni(HAm4DH)_2](NO_3)_2$ [3]}. The angle between the planes of the two thiosemicarbazone moieties is 87.3(1)°, but the Ni(II) ion lies 0.058(6) Å from one plane and 0.022(7) Å from the other. The angles between the planes of the thiosemicarbazone moieties in $[Ni(HAm4DH)_2](NO_3)_2$ and $[Ni(HAm4DH)(Am4DH)]ClO_4$ are 88.6(2)° and 84.9(2)°, respectively [3].

3.2.2. Structure of $[Zn(Am4M)(OAc)]_2$ (2)

$[Zn(Am4M)(OAc)]_2$ crystallizes as a centrosymmetric binuclear molecule with the two acetato bridging ligands in a *syn–syn* arrangement and with a Zn–Zn distance of 3.6942(7) Å. By contrast, $[Zn(Am4DH)(OAc)]_2$ has two different kinds of acetato bridge: one is *syn–syn* but the other involves just a single oxygen, as in $[Zn(Ac4E)(OAc)]_2$, where Ac4E is the anion of 2-acetylpyridine N(4)-ethylthiosemicarbazone [24]. The two Zn–O distances of $[Zn(Am4M)(OAc)]_2$, which are slightly

Table 1
Crystal and structure refinement data for, $[Ni(HAm4M)_2](ClO_4)_2\cdot 2H_2O$, $[Zn(Am4M)(OAc)]_2$ and $[Cd(HAm4M)Cl_2]\cdot DMSO$

Empirical formula	$C_{16}H_{25}Cl_2N_{10}NiO_{10}S_2$	$C_{20}H_{26}N_{10}O_4S_2Zn$	$C_{10}H_{17}CdCl_2N_5OS_2$
Colour; habit	red–brown, prism	yellow, plate	yellow, prism
Formula weight	711.19	665.37	470.71
Temperature (K)	293(2)	293(2)	293(2)
Crystal size (mm)	$0.23 \times 0.18 \times 0.11$	$0.25 \times 0.25 \times 0.10$	$0.20 \times 0.16 \times 0.08$
Diffractometer	Bruker Smart CCD 1000	Nonius CAD4	Nonius MACH3
Radiation, (λ, Å)	Mo Kα (0.71073)	Cu Kα (1.54184)	Mo Kα (0.71073)
Crystal system	monoclinic	monoclinic	triclinic
Space group	$P2_1/n$ (No. 14)	$C2/c$ (No. 15)	$P\bar{1}$ (No. 2)
Unit cell dimensions			
a (Å)	12.721(2)	26.713(3)	9.148(3)
b (Å)	16.171(2)	8.183(1)	9.856(2)
c (Å)	14.155(2)	19.568(2)	11.849(2)
a (°)	90.0	90.0	108.56(2)
β (°)	97.711(3)	131.727(6)	93.63(2)
γ (°)	90.0	90.0	112.46(1)
V (Å^3)	2885.5(6)	3192.5(5)	915.0(3)
Z	4	4	2
Density (Mg m^{-3})	1.637	1.384	1.709
Absorption coefficient (mm^{-1})	1.069	3.418	1.717
θ Range for data collection (°)	1.92–28.03	4.44–75.92	2.41–23.68
Index ranges	$-16 \le h \le 13$	$-24 \le h \le 33$	$-10 \le h \le 0$
	$-19 \le k \le 21$	$-10 \le k \le 0$	$-10 \le k \le 11$
	$-18 \le l \le 18$	$-24 \le l \le 0$	$-13 \le l \le 13$
Reflections collected	37 720	3340	2965
Independent reflections	6898 $\{R_{int} = 0.117\}$	3326 $\{R_{int} = 0.029\}$	2765 $\{R_{int} = 0.204\}$
Data/parameters	6898/382	3326/173	2765/190
Final R indices [$I > 2\sigma(I)$]	$R_1 = 0.095$, $wR_2 = 0.217$	$R_1 = 0.044$, $wR_2 = 0.121$	$R_1 = 0.059$, $wR_2 = 0.074$
R indices (all data)	$R_1 = 0.219$, $wR_2 = 0.277$	$R_1 = 0.049$, $wR_2 = 0.126$	$R_1 = 0.356$, $wR_2 = 0.109$
Goodness-of-fit	1.022	1.057	0.905
Largest difference peak and hole (e Å^{-3})	1.248 and -0.775	0.694 and -0.829	0.670 and -1.350

different, are the shortest of the five coordinating bond lengths. As in other 2-pyridyl thiosemicarbazones, the Zn–N_{im}, Zn–N_{py} and Zn–S bond lengths increase in that order. In the anionic Am4M ligand the C7–S1 bond is longer than in free HAm4M [1.750(3) Å as against 1.699(5) Å], and the N3–C7 bond (formally a double bond following loss of the proton from N3) is shorter [1.307(4) Å as against 1.358(6) Å] [6]. The other

Table 2
Selected bond lengths (Å) in $[Ni(HAm4M)_2](ClO_4)_2\cdot 2H_2O$ (**1**), $[Zn(Am4M)(OAc)]_2$ (**2**), and $[Cd(HAm4M)Cl_2]\cdot DMSO$ (**3**)

Bond	**1**	Bond	**2**	Bond	**3**
Ni1–N12	2.007(6)	Zn1–N2	2.050(2)	Cd1–N2	2.335(9)
Ni1–N22	2.005(6)	Zn1–N1	2.227(2)	Cd1–N1	2.365(10)
Ni1–N11	2.099(6)	Zn1–S1	2.370(1)	Cd1–S1	2.597(4)
Ni1–N21	2.117(6)	Zn1–O11 [a]	1.988(2)	Cd1–Cl1	2.493(4)
Ni1–S1	2.420(2)	Zn1–O12	2.020(2)	Cd1–Cl2	2.447(3)
Ni1–S2	2.416(2)				
S1–C17	1.691(9)	S1–C7	1.750(3)	S1–C7	1.692(12)
C16–N12	1.292(10)	C6–N2	1.296(3)	C6–N2	1.282(14)
N12–N13	1.396(8)	N2–N3	1.387(3)	N2–N3	1.379(11)
N13–C17	1.341(10)	N3–C7	1.307(4)	N3–C7	1.319(13)
C17–N14	1.328(9)	C7–N4	1.337(4)	C7–N4	1.328(14)
C16–N15	1.350(11)	C6–N5	1.339(3)	C6–N5	1.346(13)
S2–C27	1.670(8)				
C26–N22	1.288(9)	C11–O11	1.251(3)		
N22–N23	1.364(8)	C11–O12	1.264(3)		
N23–C27	1.386(9)				
C27–N24	1.337(10)				
C26–N25	1.349(11)				

[a] Symmetry transformation used to generate equivalent atoms: $-x, +1/2, -y+1/2, -z+1$.

Table 3
Selected bond angles (°) for $[Ni(HAm4M)_2](ClO_4)_2\cdot 2H_2O$ (**1**), $[Zn(Am4M)(OAc)]_2$ (**2**), and $[Cd(HAm4M)Cl_2]\cdot DMSO$ (**3**)

Angle	**1**			Angle	**2**	Angle	**3**
S1–Ni–N22	101.2(2)			S1–Zn1–N1	156.58(6)	S1–Cd1–N1	142.4(3)
S1–Ni–N12	82.0(2)			S1–Zn1–N2	81.87(6)	S1–Cd1–N2	75.1(3)
S1–Ni–N11	159.5(2)			S1–Zn1–Ol1 [a]	105.64(7)	S1–Cd1–Cl1	106.0(1)
S1–Ni–N21	93.5(2)			S1–Zn1–O12	102.78(6)	S1–Cd1–Cl2	107.2 (1)
S1–Ni–S2	92.8(1)			N1–Zn1–N2	74.77(8)	N1–Cd1–N2	67.4(4)
S2–Ni–N22	82.3(2)			N1–Zn1–Ol1 [a]	88.69(8)	N1–Cd1–Cl1	94.0(3)
S2–Ni1–N12	103.7(2)			N1–Zn1–O12	86.26(8)	N1–Cd1–Cl2	94.6(3)
S2–Ni1–N11	92.4(2)			N2–Zn1–Ol1 [a]	122.80(9)	N2–Cd1–Cl1	117.6(3)
S2–Ni1–N21	159.6(2)			N2–Zn1–Ol2	115.89(8)	N2–Cd1–Cl2	129.2(3)
N11–Ni1–N22	99.1(2)			Ol1 [a]–Zn1–O12	117.12(9)	Cl1–Cd1–Cl2	110.4(1)
N11–Ni1–N12	77.5(2)			O11–C11–O12	124.7(2)		
N11–Ni1–N21	88.5(2)			O11–C11–C12	117.7(3)		
N21–Ni1–N22	77.5(2)			O12–C11–C12	117.5(2)		
N21–Ni1–N12	96.3(2)			Zn1–O11 [a]–C11 [a]	130.1(2)		
N12–Ni1–N22	173.1(3)			Zn1–O12–C11	125.0(2)		
Ni1–S1–C17	96.0(3)	Ni–S2–C27	96.5(3)	Zn1–S1–C7	95.1(1)	Cd1–S1–C7	99.6(5)
Ni1–N12–C16	118.9(5)	Ni–N22–C26	120.1(5)	Zn1–N2–C6	121.4(2)	Cd1–N2–C6	120.9(9)
Ni1–N12–N13	120.7(5)	Ni–N22–N23	120.8(4)	Zn1–N2–N3	122.9(2)	Cd1–N2–N3	118.9(7)
N15–C16–N12	127.9(8)	N25–C26–N22	126.0(8)	N5–C6–N2	123.3(3)	N5–C6–N2	125.6(13)
C15–C16–N12	113.3(7)	C25–C26–N22	114.5(7)	C5–C6–N2	115.5(2)	C5–C6–N2	117.9(12)
C16–N12–N13	118.9(5)	C26–N22–N23	119.1(6)	C6–N2–N3	115.6(2)	C6–N2–N3	119.1(11)
N12–N13–C17	117.9(6)	N22–N23–C27	118.2(6)	N2–N3–C7	113.6(2)	N2–N3–C7	121.4(11)
N13–C17–N14	114.7(7)	N23–C27–N24	113.8(7)	N3–C7–N4	117.1(3)	N3–C7–N4	114.0(12)
N13–C17–S1	123.0(6)	N23–C27–S2	122.0(6)	N3–C7–S1	126.5(2)	N3–C7–S1	124.8(11)
N14–C17–S1	122.3(7)	N24–C27–S2	124.2(6)	N4–C7–S1	116.4(2)	N4–C7–S1	121.2(11)

[a] Symmetry transformation used to generate equivalent atoms: $-x,+1/2,\ -y+1/2,\ -z+1$.

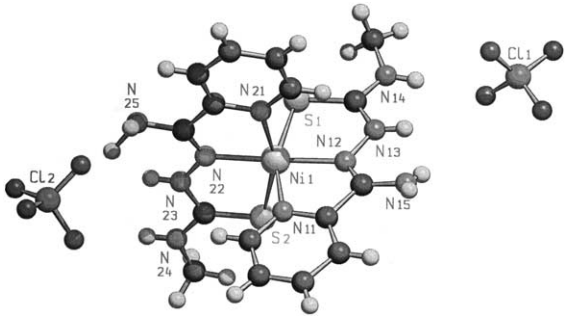

Fig. 1. Drawing of $[Ni(HAm4M)_2](ClO_4)_2$.

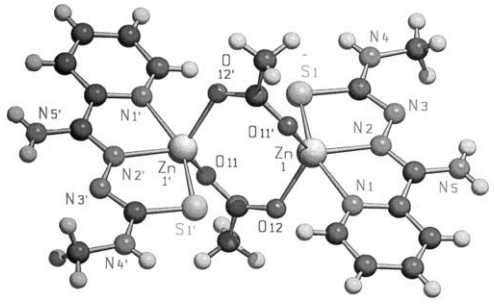

Fig. 2. Drawing of $[Zn(Am4M)(OAc)]_2$.

bond lengths in the thiosemicarbazone moiety do not differ significantly from those of HAm4M. The lengths of the two C–O bonds of the acetato groups are slightly

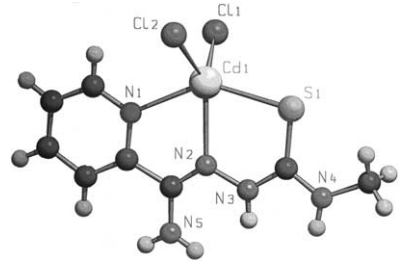

Fig. 3. Drawing of $[Cd(HAm4M)Cl_2]$.

different, in keeping with the different Zn–O distances. Compared to $[Zn(Am4DH)(OAc)]_2$, $[Zn(Am4M)(OAc)]_2$ has a significantly longer $Zn–N_{im}$ bond [2.227(2) Å as against an average 2.161(2) Å] and slightly shorter Zn–S and Zn–O distances, but the $Zn–N_{py}$ distance is the same in both compounds.

The identical ZnN_2O_2S kernels of $[Zn(Am4M)(OAc)]_2$ have N1–Zn–S angles of 156.58(6)° {cf. 150.44(5)° and 157.27(6)° for $[Zn(Am4DH)(OAc)]_2$}. With N1–Zn–S assigned as β and N1–Zn–O11′ as α, $\tau = 0.56$ [25], indicating that the arrangement about Zn is very slightly closer to a trigonal bipyramid (with N1 and S axial, and N2, O11′ and O12 equatorial) than to a square pyramid. By contrast, in $[Zn(Am4DH)(OAc)]_2$ both centres are more nearly square pyramids ($\tau = 0.20$ and 0.0), as in another recently studied binuclear zinc complex with dissimilar acetato bridges, [Zn(Ampip)-

Table 4
Hydrogen bond parameters (Å and °) in $[Ni(HAm4M)_2](ClO_4)_2\cdot 2H_2O$ (**1**), $[Zn(Am4M)(OAc)]_2$ (**2**) and $[Cd(HAm4M)Cl_2]\cdot DMSO$ (**3**)

Compound	D–H···A	d(D–H)	d(H···A)	d(D···A)	∠ (DHA)
1 [a]	N13–H13···O1#1	0.86	2.19	3.05(1)	172.1
	N14–H14···O11	0.86	2.29	3.06(1)	149.1
	N14–H14···O13	0.86	2.66	3.29(2)	131.7
	N15–H15A···O1#1	0.69	2.21	2.89(1)	165.0
	N15–H15B···O12#2	0.90	2.18	3.08(1)	174.0
	N23–H23···O22	0.86	2.12	2.97(1)	168.5
	N24–H24···O24	0.86	2.13	2.99(2)	171.5
	N25–H25A···O22	1.18	2.17	3.15(1)	137.0
	N25–25B···O14#3	0.78	2.75	3.26(2)	127.0
2 [b]	N4–H4···S1#1	0.86	2.67	3.47(3)	154.3
	N5–H5B···O12#2	0.86	2.20	2.97(3)	149.7
3 [c]	N3–H3···O2#1	0.86	1.91	2.76(1)	170.4
	N4–H4···Cl2#1	0.86	2.68	3.37(1)	137.6
	N5–H5A···O2#1	0.86	2.05	2.90(1)	171.7
	N5–H5B···Cl1#2	0.86	2.52	3.32(1)	154.1

Symmetry transformations used to generate equivalent atoms:
[a] #1: $-x+1/2$, $y+1/2$, $-z+3/2$; #2: $x-1/2$, $-y+3/2$, $z-1/2$; #3: x, y, $z-1$.
[b] #1: $-x$, y, $-z+1/2$; #2 $-x+1/2$; $y+1/2$, $-z+1/2$.
[c] #1: $-x+1$, $-y+1$, $-z+1$; #2: $-x$, $-y$, $-z+1$.

$(OAc)]_2$ (where Ampip is the anion of 2-pyridineformamide 3-piperidylthiosemicarbazone), for which $\tau = 0.04$ and 0.25 [26]. The difference between the two acetato ligands both being bis-monodentate (as in $[Zn(Am4M)(OAc)]_2$) and their one of them being bis-monodentate and the other bridging only through one oxygen (as in $[Zn(Am4DH)(OAc)]_2$ and $[Zn(Ampip)(OAc)]_2$) thus has a significant effect on the coordination polyhedra of both the zinc atoms.

There is less intermolecular hydrogen bonding in $[Zn(Am4M)(OAc)]_2$ than in other complexes of 2-pyridineformamide thiosemicarbazones because of the absence of solvate molecules. However, N4H4 interacts with a non-bonding pair of electrons on a coordinated thiolato sulfur, the N4H4···S1#1 distance and angle [3.446(3) Å and 154.3°] being similar to those found in uncomplexed N–(2-pyridyl)–N′–arylthiourea molecules [27]; and an N5 hydrogen interacts with a lone pair of electrons on a coordinated acetato oxygen atom, with a N···O distance, 2.973(3) Å, that is slightly shorter than that between an analogous nitrogen and the oxygen of a solvating water molecule in $[Zn(Am4DH)(OAc)]_2\cdot H_2O$, 3.018(3) Å [4]. As in other complexes of Am4M, the mean plane of the coordinated thiosemicarbazide moiety is just slightly inclined to that of the pyridine ring, with which it makes an angle of 3.8(2)° (Table 5).

3.2.3. Structure of $[Cd(HAm4M)Cl_2]\cdot DMSO$ (3)

A number of $[Cd(NNS)X_2]$ compounds have been reported recently (NNS being a neutral 2-pyridyl thiosemicarbazone and X being Cl, Br or I). They include $[Cd(HAm4DH)Cl_2]$ [4] and $[Cd(HAc4M)Cl_2]$ [15], where HAc4M is 2-acetylpyridine N(4)-methylthiosemicarbazone. In **3** the major ligand coordinates via its pyridine nitrogen, imine nitrogen and sulfur atoms, and the coordinating bonds between Cd and the HAm4M and chloro ligands are very similar in length to those of $[Cd(HAm4DH)Cl_2]$ [4]. The Cd–N1 and Cd–S distances are also very similar to those found in

Table 5
Characteristics of least-squares planes in $[Ni(HAm4M)_2](ClO_4)_2\cdot 2H_2O$ (**1**), $[Zn(Am4M)(OAc)]_2$, (**2**) and $[Cd(HAm4M)Cl_2]\cdot DMSO$ (**3**)

Compound	Plane	Rms dev. (Å)	Largest dev. (Å)	Angle with previous plane (°)
1	N11–C11–C12–C13–C14–15	0.0088	C14, 0.014(6)	
	C16–N12–N13–C17–S1–N14	0.0488	N12, 0.097(5)	7.1(4)
	C26–N22–N23–C27–S2–N24	0.0396	N23, 0.069(6)	87.3(1)
	N21–C21–C22–C23–C24–25	0.0053	C21, 0.008(6)	3.8(4)
2	C6–N2–N3–C7–N4–S1	0.0202	N2, 0.032(2)	
	N1–C1–C2–C3–C4–C5	0.0045	N1, 0.008(2)	3.8(2)
	N1–N2–S1	0.0000		4.4(2)
	O11–O12–C12	0.0000		89.8(2)
3	C6–N2–N3–C7–N4–S1	0.0422	N2, 0.085(9)	
	N1–C1–C2–C3–C4–C5	0.0061	C4, 0.010(9)	8.6(4)

Table 6
Distortion from square pyramidal geometry in $[Cd(NNS)Cl_2]$ complexes

Compound	β(N1–Cd1–S1)	α(N2–Cd1–Cl)	$\beta-\alpha$	$\tau=(\beta-\alpha)/60$	Ref.
$[Cd(HAm4DH)Cl_2]$ [a]	142.8	138.4	4.4	0.07	[4]
$[Cd(HAm4M)Cl_2]$	142.4	129.2	13.2	0.22	this work
$[Cd(HAmpip)Cl_2]$ [b]	134.6	137.9	3.3	0.06	[26]
$[Cd(HAc4DH)Cl_2]$ [c]	141.5	137.7	3.8	0.06	[28]
$[Cd(HAc4M)Cl_2]$ [d]	139.8	136.7	3.1	0.05	[15]
$[Cd(HAc4DM)Cl_2]$ [e]	145.2	135.5	9.7	0.16	[29]

[a] HAm4DH = 2-pyridineformamide thiosemicarbazone.
[b] HAmpip = 2-pyridineformamide 3-piperidylthiosemicarbazone.
[c] HAc4DH = 2-acetylpyridine thiosemicarbazone.
[d] HAc4M = 2-acetylpyridine N(4)-methylthiosemicarbazone.
[e] HAc4DM = 2-acetylpyridine N(4)-dimethylthiosemicarbazone.

$[Cd(HAc4M)Cl_2]$ [15], but the Cd–N2 distance is significantly shorter than in the latter [2.365(10) Å as against 2.432(2) Å], showing that electron donation by the formamide NH_2 is significantly greater than that of the acetyl CH_3. This difference is probably responsible for the Cd–Cl bond being somewhat longer in $[Cd(HAm4M)Cl_2]$. Like all other $[Cd(NNS)Cl_2]$ compounds, $[Cd(HAm4M)Cl_2]$ has a square pyramidal coordination polyhedron, but it also exhibits greater distortion towards trigonal bipyramidal stereochemistry than any other known compound of this type (Table 6).

In the thiosemicarbazone moiety the only bond of $[Cd(HAm4M)Cl_2]$ to differ significantly in length from the corresponding bonds of $[Cd(HAm4DH)Cl_2]$ [4] and $[Cd(HAc4M)Cl_2]$ [15] is N3–C7 {1.319(13) Å in $[Cd(HAm4M)Cl_2]$, 1.358(6) Å in $[Cd(HAm4DH)Cl_2]$ and 1.370 Å in $[Cd(HAc4M)Cl_2]$}. The mean planes of the pyridine ring and the thiosemicarbazide chain make an angle of 8.6(4)° {cf. 2.0(2)° in $[Cd(HAm4DH)Cl_2]$}.

2-Pyridineformamide thiosemicarbazones have more possibilities of hydrogen bonding than 2-formyl-, 2-acetyl- and 2-benzoylpyridine thiosemicarbazones because of the presence of the formamide NH_2 group. In the present case, the four hydrogen bonds of $[Cd(HAm4M)Cl_2]\cdot DMSO$ (N3H3 and N5H5A with the oxygen of a neighbouring DMSO, N4H4 with the corresponding Cl2, and N5H5B with Cl1 of another neighbouring molecule; see Table 4) may be compared with the two of $[Cd(HAc4M)Cl_2]\cdot 2DMSO$, in which it is N3H3 and N4H4 that both interact with the same DMSO oxygen.

4. Supplementary material

Crystallographic data for the structures reported in this paper (excluding structure factors) have been deposited with the Cambridge Crystallographic Data Centre, CCDC Nos. 168861 (for $[Ni(HAm4M)_2](ClO_4)_2\cdot 2H_2O$), 168862 (for $[Zn(Am4M)(OAc)]_2$) and 168863 (for $[Cd(HAm4M)Cl_2]\cdot DMSO$). Copies of this information may be obtained free of charge from The Director, CCDC, 12 Union Road, Cambridge, CB2 1EZ, UK (fax: +44-1223-336033; e-mail: deposit@ccdc.cam.ac.uk or www: http://www.ccdc.cam.ac.uk).

References

[1] A. Castiñeiras, I. Garcia, E. Bermejo, D.X. West, Z. Naturforsch., Teil B 55 (2000) 511.
[2] A. Castiñeiras, I. Garcia, E. Bermejo, D.X. West, Polyhedron 19 (2000) 1873.
[3] A. Castiñeiras, I. Garcia, E. Bermejo, K.A. Ketcham, D.X. West, manuscript in preparation.
[4] A. Castiñeiras, I. Garcia, E. Bermejo, D.X. West, manuscript in preparation.
[5] D.X. West, J.K. Swearingen, A.K. El-Sawaf, Transition Met. Chem. 25 (2000) 87.
[6] D.X. West, J.K. Swearingen, J. Valdés-Martínez, S. Hernández-Ortega, A.K. El-Sawaf, F. van Meurs, A. Castiñeiras, I. Garcia, E. Bermejo, Polyhedron 18 (1999) 2919.
[7] Bruker, SMART and SAINT. Area Detector Control and Integration Software, Bruker Analytical X-ray Instruments Inc., Madison, WI, USA, 1997.
[8] G.M. Sheldrick, SADABS. Program for Empirical Absorption Correction of Area Detector Data. University of Göttingen, Göttingen, Germany, 1997.
[9] A.C.T. North, D.C. Phillips, F.S. Mathews, Acta Crystallogr., Sect. A 24 (1968) 351.
[10] G.M. Sheldrick, SHELXL-97. Program for the Refinement of Crystal Structures, University of Göttingen, Göttingen, Germany, 1997.
[11] International Tables for X-ray Crystallography, Vol. C, Kluwer Academic Publishers, Dordrecht, The Netherlands, 1995.
[12] E. Keller, SCHAKAL97. A computer program for the graphic representation of molecular and crystallographic models, University of Freiburg, Germany, 1997.
[13] G. Bojesen, Org. Mass. Spectrom. 20 (1985) 413.
[14] M.F. Iskander, L. El-Sayed, M.A. Lasheem, Inorg. Chim. Acta 16 (1976) 147.
[15] E. Bermejo, R. Carballo, A. Castiñeiras, R. Domínguez, A.E. Liberta, C. Maichle-Mössmer, M.M. Salberg, D.X. West, Eur. J. Inorg. Chem. (1999) 965.
[16] M.B.elicchi Ferrari, S. Capacchi, F. Bisceglie, G. Pelosi, P. Tarasconi, Inorg. Chim. Acta 32 (2001) 81.
[17] D.K. Rastoh, K.C. Sharma, J. Inorg. Nucl. Chem. 36 (1974) 2219.

[18] (a) K. Nakamoto, Infrared and Raman Spectra of Inorganic and Coordination Compounds, Wiley, New York, 1986;
(b) J. Weidlein, U. Müller, K. Dehnicke, Schwingungsfrequenzen II, Thieme Verlag, Stuttgart, 1986.
[19] H. Ackermann, F. Weller, B. Neumüller, K. Dehnicke, Z. Anorg. Allg. Chem. 625 (1999) 147.
[20] A. Castiñeiras, R. Carballo, T. Perez, Polyhedron 20 (2001) 441.
[21] W.J. Geary, Coord. Chem. Rev. 7 (1971) 81.
[22] A.B.P. Lever, Inorganic Electronic Spectroscopy, Elsevier, New York, 1984.
[23] T. Drakenberg, N.-O. Björk, R. Portanova, J. Phys. Chem. 82 (1978) 2423.
[24] L. Bresolin, R.A. Burrow, M. Hörner, E. Bermejo, A. Castiñeiras, Polyhedron 16 (1997) 3947.
[25] A.W. Addison, T.N. Rao, J. Reedijt, J. van Rijn, G.C. Verschoor, J. Chem. Soc., Dalton Trans. (1984) 1349.
[26] A. Castiñeiras, I. Garcia, E. Bermejo, K.A. Ketcham, A.K. El-Sawaf, D.X. West, unpublished results.
[27] (a) J. Valdés-Martínez, S. Hernández-Ortega, D.X. West, L.J. Ackerman, J.K. Swearingen, A.K. Hermetet, J. Mol. Struct. 478 (1999) 219;
(b) D.X. West, J.K. Swearingen, A.K. Hermetet, L.J. Ackerman, C. Presto, J. Mol. Struct. 522 (2000) 27;
(c) J. Valdés-Martínez, S. Hernández-Ortega, L.J. Ackerman, D.T. Le, J.K. Swearingen, D.X. West, J. Mol. Struct. 524 (2000) 51.
[28] J.S. Casas, M.V. Castaño, M.S. Garcia-Tasende, I. Martínez-Santamarta, J. Sordo, E.E. Castellano, J. Zuckerman-Schpector, J. Chem. Res. (S) (1992) 324; (M) (1992) 2626.
[29] E. Bermejo, R. Carballo, A. Castiñeiras, R. Domínquez, C. Maichle-Mössmer, A.E. Liberta, D.X. West, Z. Naturforsch., Teil B 54 (1999) 777.